Quiescent-Interval Single-Shot Unenhanced Magnetic Resonance Angiography of Peripheral Vascular Disease: Technical Considerations and Clinical Feasibility

Robert R. Edelman,[1]* John J. Sheehan,[1] Eugene Dunkle,[1] Nancy Schindler,[2] James Carr,[3] and Ioannis Koktzoglou[1]

We performed technical optimization followed by a pilot clinical study of quiescent-interval single-shot MR angiography for peripheral vascular disease. Quiescent-interval single-shot MR angiography acquires data using a modified electrocardiographic (ECG)-triggered, fat suppressed, two-dimensional, balanced steady-state, free precession pulse sequence incorporating slice-selective saturation and a quiescent interval for maximal enhancement of inflowing blood. Following optimization at 1.5 T, a pilot study was performed in patients with peripheral vascular disease, using contrast-enhanced MR angiography as the reference standard. The optimized sequence used a quiescent interval of 228 ms, $\alpha/2$ catalyzation of the steady-state magnetization, and center-to-out partial Fourier acquisition with parallel acceleration factor of 2. Spatial resolution was 2-3mm along the slice direction and 0.7-1mm in-plane before interpolation. Excluding stented arterial segments, the sensitivity, specificity, and positive and negative predictive values of quiescent-interval single-shot MR angiography for arterial narrowing greater than 50% or occlusion were 92.2%, 94.9%, 83.9%, and 97.7%, respectively. Quiescent-interval single-shot MR angiography provided robust depiction of normal peripheral arterial anatomy and peripheral vascular disease in less than 10 min, without the need to tailor the technique for individual patients. Moreover, the technique provides consistent image quality in the pelvic region despite the presence of respiratory and bowel motion. Magn Reson Med 63:951–958, 2010. © 2010 Wiley-Liss, Inc.

Key words: magnetic resonance angiography unenhanced; flow; peripheral vascular disease; steady-state precession; two dimensional

Peripheral vascular disease (PVD) has an age-adjusted prevalence of 12% in the United States, causes significant morbidity, and is associated with excess cardiovascular mortality (1,2). Contrast-enhanced (CE) magnetic resonance angiography (MRA) often substitutes for the more invasive "gold standard" procedure of digital subtraction angiography (3). Given the frequency of renal functional impairment in patients with PVD and concerns about nephrogenic systemic fibrosis, there is growing interest in unenhanced MRA (4,5).

Two-dimensional time of flight (2DTOF) has been extensively evaluated for unenhanced MRA of the lower extremities (6–8). However, the method is too slow for many patients to tolerate, is sensitive to patient motion, and suffers from flow artifacts within horizontally oriented vessel segments. Over the last few years, several "next-generation" unenhanced MRA techniques have been introduced. Of these, fresh blood imaging (FBI) has undergone the most clinical validation. FBI is a subtractive technique that uses a three-dimensional half-Fourier turbo spin-echo pulse sequence in conjunction with selective application of flow-dephasing gradients in order to ensure that signal from rapidly flowing arterial spins is fully suppressed (9). Initial clinical studies demonstrate considerable clinical promise, with excellent image quality in healthy subjects. In one study using 16-slice CT angiography as the reference standard, accuracy was 94% (10). However, a fundamental challenge is the need to calibrate the trigger delay and flow-dephasing gradients for individual patients and vessel segments. The systolic image data must be acquired exactly during the brief period of peak arterial flow. However, the onset of peak flow is delayed in distal arterial segments compared with proximal ones, and the timing is altered by the presence of stenotic lesions. A recent clinical trial of FBI for the peripheral arteries reported serious artifacts in approximately 47% of the patients, resulting from motion, inaccurate trigger delays, and vessel blurring (11). Moreover, one cannot always be certain whether a loss of vessel signal or narrow vessel caliber is due to disease or is merely an artifact of using the wrong amplitude for the flow-spoiling gradients or an incorrect trigger delay.

Motion sensitivity is another concern. Our experience with 2DTOF and FBI has been that neither is reliable for imaging of the pelvic arteries due to respiratory and bowel motion. FBI requires the subtraction of two three-dimensional data sets that are acquired sequentially over several minutes. The motion sensitivity is problematic, given that the iliac arteries are a common location for stenotic disease in patients with claudication.

An ideal methodology for unenhanced MRA should be fast, easy to use, and insensitive to patient motion, heart rate, and flow patterns. For this purpose, we have implemented quiescent-interval single-shot (QISS) MRA, which acquires data using a modified single shot two-dimensional balanced steady-state free precession pulse sequence (12). Unlike subtractive unenhanced three-

[1]Department of Radiology, NorthShore University HealthSystem, Evanston, Illinois, USA

[2]Department of Surgery, NorthShore University HealthSystem, Evanston, Illinois, USA

[3]Northwestern Radiology and the Feinberg School of Medicine, Northwestern University, Chicago, Illinois, USA

*Correspondence to: Robert R. Edelman, M.D., Department of Radiology, NorthShore University HealthSystem, 2650 Ridge Ave., Evanston, IL 60201. E-mail: redelman@northshore.org

Received 28 July 2009; revised 18 September 2009; accepted 21 October 2009.

DOI 10.1002/mrm.22287
Published online in Wiley InterScience (www.interscience.wiley.com).

dimensional MRA methods, the imaging parameters for QISS MRA require minimal if any tailoring for individual patients. The technique was optimized in healthy subjects and then evaluated with a pilot study of patients with PVD using CE-MRA as the reference standard.

MATERIALS AND METHODS

The study was approved by the institutional review board, and written informed consent was obtained from all subjects. A series of healthy subjects without known PVD (ages 20-66) and eight patients (eight male, ages 56-90) with documented PVD were studied. Patients with estimated glomerular filtration rate (eGFR) <30 mL/min/1.73 m^2 were excluded from participation to avoid risk of nephrogenic systemic fibrosis. Imaging was performed on a 1.5-T MR scanner (MAGNETOM Avanto; Siemens Healthcare, Erlangen, Germany). The system is equipped with 32 radiofrequency (RF) receiver channels and a gradient system capable of 45 mT/m maximum strength and 200-μs rise time from 0 mT/m to 45 mT/m. Multielement peripheral vascular coils and spine array coils were used to receive the MR signal. A ninth patient (male, 67 years old) referred after a CE-MRA study at another institution was included for demonstration purposes but was excluded from the pilot data analysis since different imaging parameters were used for the CE-MRA.

QISS MRA is illustrated in Fig. 1 and can be summarized as follows:

1. Following a user-selected time delay after the R-wave, a slice-selective saturation RF pulse is applied to the imaging slice to set the longitudinal magnetization of tissues within the slice to zero.
2. A tracking saturation RF pulse is applied caudally.
3. Next there is a quiescent interval (QI), roughly coinciding with the period of rapid systolic arterial flow, during which no RF pulses are applied.
4. A chemical shift-selective fat saturation RF pulse is followed by an RF catalyzation sequence to force the magnetization of in-plane spins toward the steady-state value.
5. A single-shot two-dimensional balanced steady-state free precession pulse sequence is used to image arterial spins within the slice during diastole, when flow is slow or absent.
6. The entire process is repeated for the next slice, with the acquisition order being sequential from bottom to top.

Technical Optimization

Technical comparisons made during the optimization process included the following: (a) ECG gating versus pulse gating; (b) linear versus $\alpha/2$ RF catalyzation; (c) 5/8 partial Fourier using center-to-out trajectory versus out-to-center trajectory; (d) full Fourier; and (e) flip angle of 0°, 90°, and 180° for the preparatory slice-selective RF pulse. In one subject, QISS MRA using 90° and 180° preparatory slice-selective RF pulses respectively were reacquired using a pulse repetition time (TR) of 1 sec (versus the usual TR of 714 ms), which was approximately equal to the R-R interval in this subject. Given normal respiratory variation in the R-R interval, this choice of TR deliberately caused some slices to be acquired every heartbeat and others to be acquired every other heartbeat in an unpredictable manner.

The optimized QISS pulse sequence for rapid scanning of the lower extremities used the following imaging parameters: TR/echo time/QI/flip angle = 3.0 ms/1.4 ms/228 ms/90°, time delay = 100 ms, 2.4mm effective slice thickness (3.0mm with 0.6mm overlap), parallel acceleration factor of 2, bandwidth 676-694 Hz/pixel, flip angle of 135° for the fat suppression pulse. The acquisition matrix ranged from 352-400, depending on field of view (34-40 cm), maintaining in-plane spatial resolution at 1mm (interpolated to 0.5mm). Eight groups of 60 slices were acquired to span the peripheral arteries from the level of the distal aorta to the pedal arteries. For a heart rate of 60 beats/min, scan time was 1 min per slice group, so that total scan time was approximately 8 min. In some subjects, additional high-resolution imaging was performed using a slice thickness of 2mm and in-plane resolution of 0.7mm (interpolated to 0.35mm).

Limited comparisons were made with standard ECG-gated 2DTOF MRA (slice thickness = 3mm, in-plane resolution = 1mm, 128 axial slices with 20% overlap, tracking presaturation, field of view 170mm × 340mm, gated to each R-R interval, echo time = 5.5 ms with flow compensation in slice and read directions, 6/8 partial Fourier, minimum TR = 493 ms, approximately 5 sec per slice). QISS and 2DTOF MRA were compared in healthy subjects and a programmable pulsatile flow phantom (CompuFlow 1000 MR; Shelley Medical Imaging Technologies, London, Ontario, Canada) using a blood-mimicking fluid (T_1 = 850 ms, T_2 = 170 ms).

Data Acquisition: CE-MRA

The hybrid protocol consisted of a time-resolved CE-MRA through the calf and stepping table MRA for the remainder of the peripheral vascular system. The contrast agent was either gadopentetate dimeglumine (Bayer, Berlin, Germany) or gadobenate dimeglumine (Bracco Imaging, Milan, Italy) administered intravenously followed by a saline chaser. A time-resolved coronal acquisition was obtained through the calf and proximal foot using a multiphase time-resolved angiography with interleaved stochastic trajectories acquisition (13), injection rate of 2 mL/sec for 5-8 mL of contrast agent, parallel acceleration factor of 2, TR/echo time = 3 ms/1 ms, spatial resolution of 1.9mm (slice thickness) × 1.1mm × 1.3mm, 9.6 sec/phase. For the stepping table acquisition, a 1- to 2-mL test bolus was used to determine timing. Three stations were acquired pre- and postcontrast using TR/echo time/flip angle = 3 ms/1 ms/20°, 50-cm field of view, slice thickness of 1.5mm, in-plane spatial resolution of 1mm × 1mm, parallel acceleration factor of 2, 22 sec per station. A dual-phase infusion protocol administered 0.14 mmol/kg of the contrast agent, initially at 1.5 mL/sec, followed by 0.6 mL/sec. The subtracted images were processed using a maximum intensity projection for

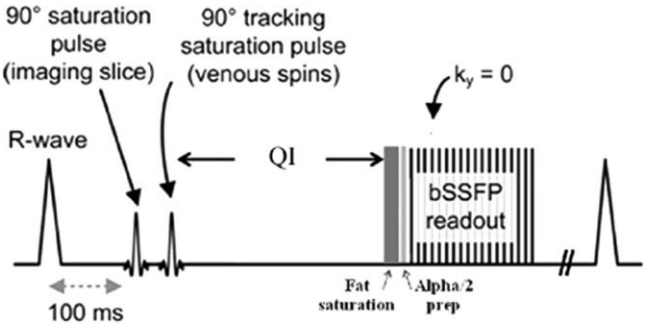

FIG. 1. Pulse sequence diagram for QISS MRA.

interpretation. Breath holding was used for the pelvic station only.

Image Analysis

Images were viewed and processed on a Leonardo workstation (Siemens Healthcare, Erlangen, Germany) using standard three-dimensional reconstruction software. The arterial tree was classified into the following 31 segments: segment 1, infrarenal aorta; segments 2 and 3, right and left common iliac arteries, respectively; segments 4 and 5, right and left external iliac arteries, respectively; segments 6 and 7, right and left common femoral arteries, respectively; segments 8 and 9, proximal half of right and left superficial femoral arteries, respectively; segments 10 and 11, distal half of right and left superficial femoral arteries, respectively; segments 12 and 13, right and left popliteal arteries, respectively; segments 14 and 15, right and left tibioperoneal trunk, respectively; segments 16 and 17, proximal half of right and left anterior tibial arteries, respectively; segments 18 and 19, distal half of right and left anterior tibial arteries, respectively; segments 20 and 21, proximal half of right and left peroneal arteries, respectively; segments 22 and 23, distal half of right and left peroneal arteries, respectively; segments 24 and 25, proximal half of right and left posterior tibial arteries, respectively; segments 26 and 27, distal half of right and left posterior tibial arteries, respectively; segments 28 and 29, right and left dorsal pedal arteries, respectively; and segments 30 and 31, right and left medial plantar arteries, respectively.

FIG. 2. Full-thickness anteroposterior maximum intensity projection from QISS MRA acquired in approximately 8 min using eight stations, each with 60 slices. Note the comprehensive visualization of the arterial system, with excellent suppression of veins and background tissues.

FIG. 3. Two views of a high-resolution (2mm × 0.7mm) QISS MRA focused to the left calf. There is excellent depiction of the muscular branches about the knee and the distal vessels.

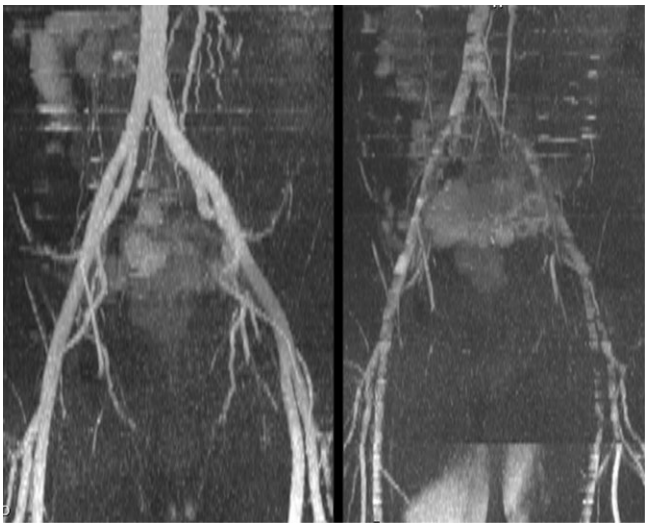

FIG. 4. Comparison of QISS MRA acquired in the pelvis with ECG gating and a time delay of 100 ms (left) versus pulse gating and a time delay of 0 (right). Note the dramatic worsening in image quality with pulse gating because the QI for inflow mainly overlaps the period of slow and/or reversed diastolic flow, whereas with ECG gating the QI mainly overlaps rapid forward systolic flow.

The arterial segments of the eight patients were assessed for the presence of vascular disease. The degree of stenosis for each vascular segment was defined by using a four-point scale (grade 0, normal; grade 1, luminal narrowing less than or equal to 50%; grade 2, luminal narrowing >50% but no occlusion; or grade 3, occlusion). When two or more stenoses were present in one segment, the most severe lesion was used for subsequent assignment of a grade and analysis.

Statistical Analysis

Statistical software (SPSS, version 17.0; SPSS Inc., Chicago, IL) was used to perform the statistical analyses. Concordance of degree of stenosis scores between CE-MRA and QISS MRA was assessed using Cohen κ analysis. A P value less than 0.05 was assumed to indicate statistical significance. Sensitivity, specificity, and positive predictive and negative predictive values for QISS MRA were computed using CE-MRA as the standard of reference examination.

RESULTS

An example of a whole-leg QISS MRA is given in Fig. 2 and high-resolution QISS MRA of the calf, in Fig. 3. Main and branch arterial conspicuity was excellent, and there was uniform background signal, as well as near-total venous suppression.

Technical Optimization

ECG gating was superior to pulse gating. With pulse gating, the QI substantially overlapped the period of slow or reversed diastolic flow, causing a loss of intravascular signal (Fig. 4). An $\alpha/2$ RF catalyzation (Fig. 5a) showed only minimally better fat suppression than a linear catalyzation (Fig. 5b). The image quality difference for the two partial Fourier trajectories was more dramatic; a center-to-out partial Fourier trajectory showed much better fat suppression than an out-to-center trajectory (Fig. 5c) due to the reduced number of RF pulses between the application of fat saturation and the center of k-space. A full Fourier acquisition (Fig. 5d) gave inferior fat suppression to a partial Fourier acquisition. With no preparatory slice-selective RF pulse, background suppression was nonuniform and veins were more prominent (Fig. 5e). Suppression of muscle signal was greater with a 180° flip angle for the preparatory slice-selective RF pulse (Fig. 5f) than a 90° flip angle. However, use of a 180° flip angle made the technique more sensitive to variations in heart rate compared with a 90° flip angle (Fig. 5g).

Compared with 2DTOF at comparable slice thickness and in-plane spatial resolution, QISS MRA quality was

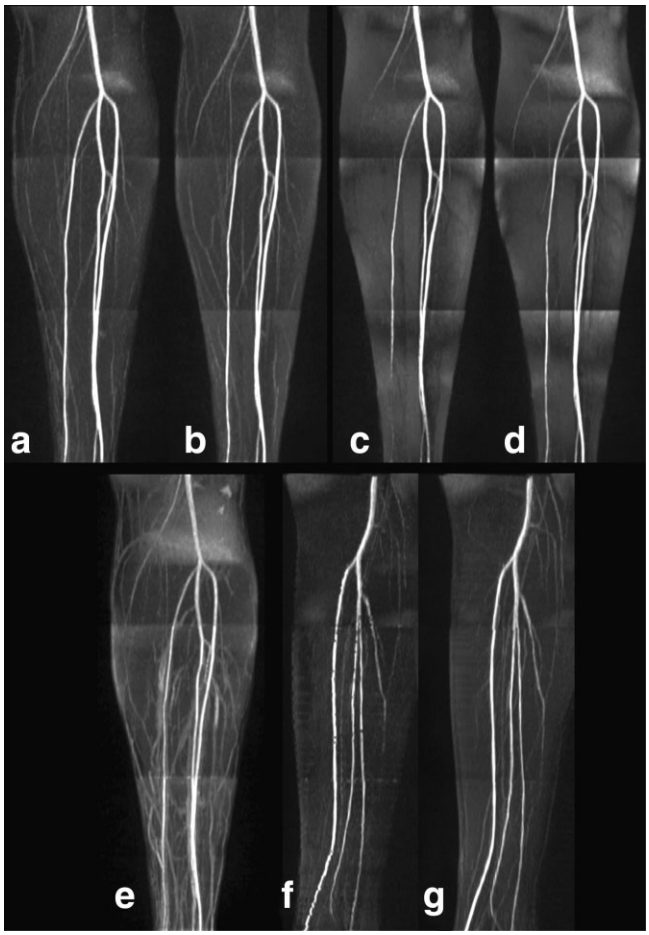

FIG. 5. Technical optimization. **a:** The optimal parameters consisted of an $\alpha/2$ RF catalyzation, center-to-out 5/8 partial Fourier trajectory, 90° flip angle for the preparatory slice-selective RF pulse; **(b)** linear catalyzation; **(c)** out-to-center partial Fourier trajectory; **(d)** full Fourier acquisition; **(e)** no preparatory slice-selective RF pulse; **(f)** 180° flip angle for the preparatory slice-selective RF pulse with gating varying between one and two R-waves; **(g)** 90° flip angle for the preparatory slice-selective RF pulse with gating varying between one and two R-waves.

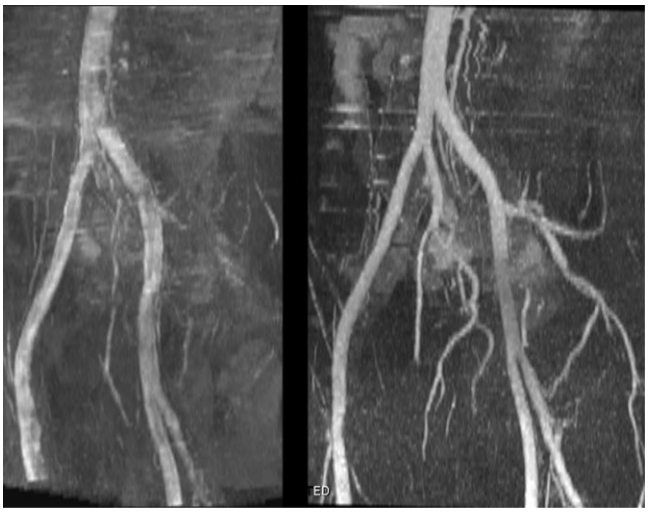

FIG. 6. Comparison of right posterior oblique views of 2DTOF MRA through the pelvis (left) (128 3mm-thick slices acquired in approximately 7 min) and a two-station QISS MRA (right) (120 3mm-thick slices acquired in approximately 2 min). Vessel uniformity and branch detail are markedly better with QISS.

superior, motion artifacts were reduced, and scan time was much shorter (Fig. 6).

Initial evaluation of QISS MRA in a pulsatile flow phantom demonstrated excellent flow contrast over a wide range of velocities (Fig. 7). Compared with 2DTOF, maximal signal was reached at substantially lower peak velocities using QISS MRA. For instance, at a 3mm slice thickness, QISS signal was maximal at about 10 cm/sec, whereas 2DTOF signal was maximal at about 34 cm/sec.

Pilot Clinical Study

In all subjects, QISS MRA demonstrated the entire length of the peripheral vascular tree from aorta to pedal vessels. Arterial anatomy was accurately demonstrated both proximal and distal to stenotic disease, without the need to modify any of the acquisition parameters (Figs. 8 and 9). Many of the collateral vessels were also well shown (Fig. 10), although not always as completely as with CE-MRA.

In one patient with tortuous pelvic vessels, some artifactual signal decrease was observed focally in the left external iliac artery, likely due to the effect of the caudally positioned tracking saturation RF pulse on superiorly directed arterial flow within the tortuous segment. By reacquiring a QISS MRA slice group (1-min scan time) using a tilted rather than axial orientation, the full intravascular signal was recovered.

Two patients had atrial arrhythmias. Despite the irregular variation in the R-R interval, no image degradation was observed in QISS MRA.

All of the 112 arterial segments deemed assessable by CE-MRA in the four volunteers were assessable by QISS MRA, while 225 out of 231 arterial segments considered to be assessable by CE-MRA in patients with PVD were assessable by QISS MRA. Four of the six arterial segments unassessable by QISS MRA occurred in the right and left common and external iliac arteries of a patient with bilateral iliac stents. A remaining unassessable segment occurred in the same patient near a surgical clip located at the origin of a superficial femoral artery bypass graft, while the final unassessable segment was observed in the right common iliac artery of a separate volunteer.

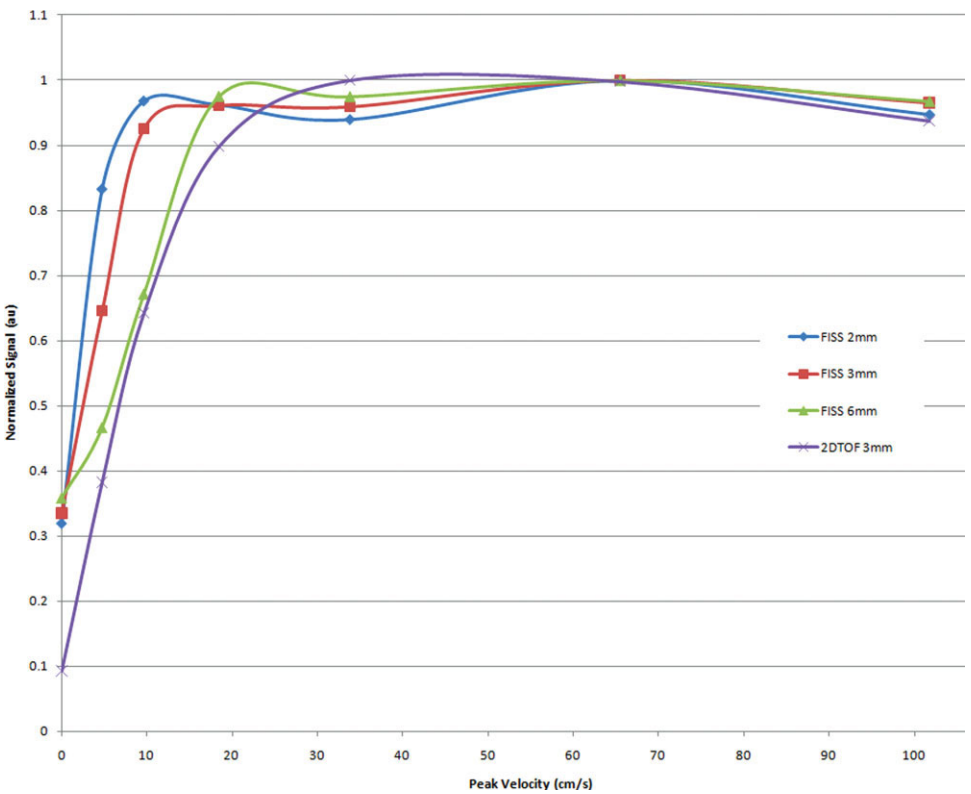

FIG. 7. Relationship of signal to flow velocity for QISS (slice thicknesses of 2mm to 6mm) and 2DTOF (slice thickness 3mm) in a pulsatile flow phantom. The flow phantom had a triphasic waveform mimicking the pattern of normal peripheral arterial blood flow with a simulated heart rate of 71 beats/min. Note that the flow signal is approximately constant for QISS over nearly the full range of tested velocities, whereas the flow signal for 2DTOF drops precipitously for velocities less than 30 cm/sec. This helps to explain the observation in Fig. 6 that small branches and distal vessels, which have lower flow velocities than the larger proximal arteries, are not well shown with 2DTOF.

FIG. 8. QISS MRA (left) versus CE-MRA (right) in a patient with vessel ectasia and mild multifocal disease. There is good correspondence between the two imaging tests. On the full-thickness MIP of the QISS MRA, a small focus of signal decrease was observed in the proximal left superficial femoral artery but appeared normal on thin-section MIPs (not shown).

Out of the 231 arterial segments viewed with CE-MRA in patients, 116 were characterized as being normal. Of the remaining 115 arterial segments 61, 27, and 27 arterial segments were characterized as having arterial narrowing of less than or equal to 50%, arterial narrowing of greater than 50%, and complete occlusion, respectively. By comparison, 66, 29, and 28 arterial segments were deemed by QISS MRA as having less than or equal to 50% luminal narrowing, greater than 50% luminal narrowing, and complete occlusion, respectively. These findings are summarized in Table 1.

Considering CE-MRA as the standard of reference examination, the sensitivity and specificity values of QISS MRA for detecting arterial occlusion or narrowing greater than 50% were 87.0% and 94.9%, respectively. For these lesions, the positive predictive value and negative predictive value for QISS MRA were 83.9% and 96%, respectively. Excluding the iliac segments in the patient with bilateral iliac stents, sensitivity, specificity, positive predictive value, and negative predictive values of QISS MRA for arterial narrowing greater than 50% or occlusion were 92.2%, 94.9%, 83.9%, and 97.7%, respectively. There was excellent agreement between the degree of stenosis scores obtained with QISS MRA and CE-MRA ($\kappa = 0.79$).

DISCUSSION

QISS MRA is not a flow-independent technique like some that have been previously described (14,15). For instance, it is obviously sensitive to flow direction and vascular signal is suppressed when there is no flow. However, QISS is nonetheless robust to a wide range of flow patterns and velocities, as was initially demonstrated in a pulsatile flow phantom where maximal signal intensity was observed with peak velocities as low as 10 cm/sec. The robustness was confirmed in vivo with the observation that intravascular signal did not appear

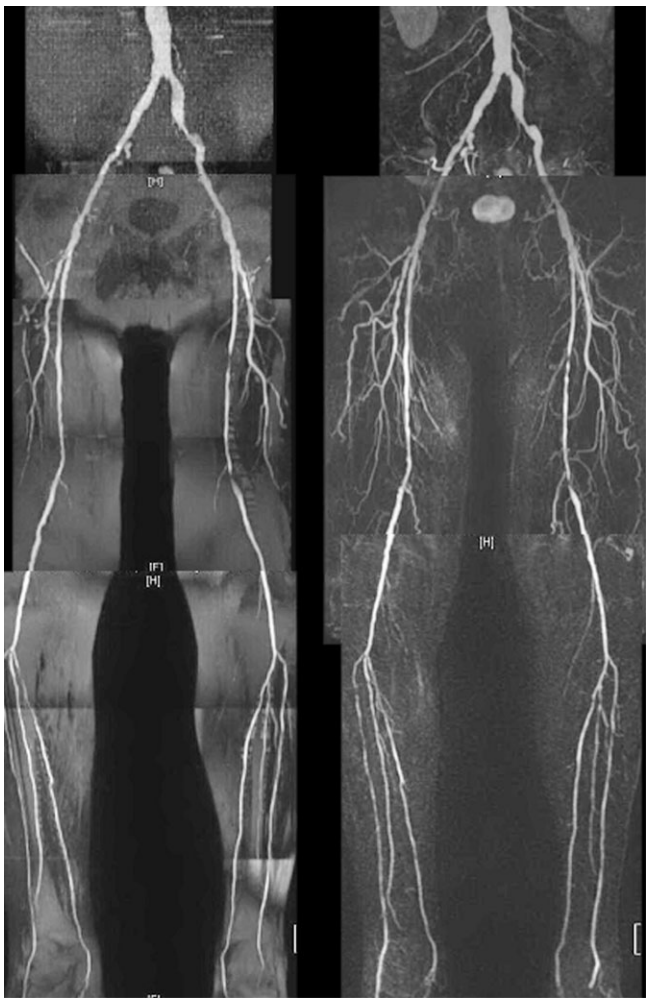

FIG. 9. Patient with moderately severe multifocal disease. There is overall good correspondence between QISS MRA (left) and CE-MRA (right). With QISS, there is slight exaggeration of the extent of a short-segment occlusion involving the proximal left superficial femoral artery, but the grade of the lesion is not affected.

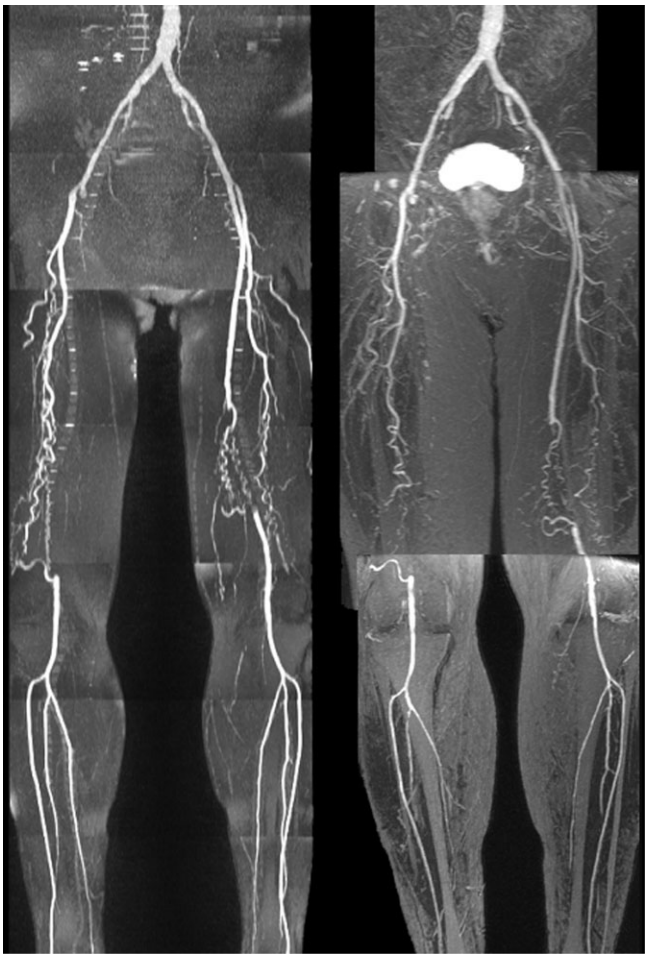

FIG. 10. Patient with bilateral superficial femoral artery occlusions. Despite the severity of disease, QISS MRA (left) correlates well with the CE-MRA (right), shows most of the collateral vessels, and better shows the calf vessels than the CE study.

to vary substantially between healthy arterial segments and ones with severe disease (including collateral vessels) where flow was particularly slow. The basis is that unsaturated arterial spins translate only a short distance (~3mm) to enter the slice where their signals are acquired. The inflow of arterial spins occurs during the QI, when no RF pulses are applied. This feature ensures that flow saturation is minimal. Moreover, the QI is timed to coincide with the period of rapid systolic arterial inflow. The relatively long duration of the QI provides sufficient leeway that there was little if any need to individually calibrate the sequence timing for each subject. In contrast, with FBI it is essential to determine the precise timing of peak arterial flow for each vessel segment. With FBI, it may also be necessary to incorporate flow-spoiling gradients to improve sensitivity for distal or diseased vessel segments where flow velocities are reduced.

Only two of our patients had significant cardiac arrhythmias, so it is not possible to make any generalizations. However, in these patients QISS MRA quality was excellent and tissue signal was uniform across all slices despite an irregular heart rhythm. The signal uniformity derives from the application of a slice-selective saturation RF pulse that resets the longitudinal magnetization of all tissues within the slice to zero, irrespective of the R-R interval. The longitudinal recovery of the background tissues is then determined by the value of QI, which is constant. On the other hand, 2DTOF, FBI, and related subtractive unenhanced MRA methods are intolerant of cardiac arrhythmias (which are common in the elderly) since the background signal inevitably varies with the R-R interval.

Several technical improvements were implemented over the course of the study. For instance, we initially tried a linear ramp RF catalyzation for the balanced steady-state free precession readout and a standard (out-to-center) partial Fourier acquisition. By replacing the linear ramp with an $\alpha/2$ RF catalyzation (16,17) and using a center-out partial Fourier acquisition, the number of RF pulses interposed between the fat saturation pulse and the center of *k*-space was minimized, thereby improving the quality of fat suppression. It is notable that excellent fat suppression was obtained without the need for image subtraction or multiecho acquisitions, which would have increased scan time or worsened the sensitivity to motion or flow artifact. With better fat suppression, branch vessels, collaterals, and distal vessels in the calf were more clearly depicted. Given the reduced number of RF pulses applied with parallel imaging and partial Fourier, SAR was not a limiting factor despite the use of a large flip angle and balanced SSFP readout.

One of the biggest challenges for unenhanced MRA techniques is motion artifact in the pelvis. Although respiratory motion in the pelvis is modest compared with the abdomen, it is present to a variable extent in most subjects. Both 2DTOF and unenhanced subtractive MRA methods tend to be unreliable in the presence of respiratory or bowel motion. For subtractive methods, two data sets are acquired sequentially over several minutes, so that any motion produces misregistration artifacts. Unfortunately, these three-dimensional methods do not

Table 1
Degree of Stenosis Scores for Arterial Segments

QISS MRA	CE-MRA				
	No stenosis	≤50% stenosis	>50% stenosis	Occlusion	Total
No stenosis	100	2	0	0	102
≤50% stenosis	12	50	4	0	66
>50% stenosis	4	5	18	2	29
Occlusion	0	1	2	25	28
Total	116	58	24	27	225

allow data acquisition within a single breath-holding period, nor is breath holding practical with more traditional 2DTOF MRA methods. QISS is less sensitive to motion than these other techniques because it uses a single-shot, nonsubtractive acquisition. Nonetheless, if motion artifact is excessive, then breath holding is an option so long as a reduced number of slices (e.g., 20) are acquired at a time. Alternatively, navigator gating techniques could be applied. Bowel peristalsis was found to cause minimal if any artifact with QISS. Although not a limitation in this study, given the use of a balanced SSFP readout one can anticipate that off-resonance artifacts might occur in patients who have excessive amounts of air-filled bowel directly adjacent to blood vessels.

Although we did not perform a rigorous comparison of QISS MRA with 2DTOF and FBI in our patient cohort, the consistency with which QISS MRA depicted all vessel segments irrespective of disease severity suggests that it may offer substantial clinical advantages compared with these other techniques. Use of 2DTOF for the peripheral vasculature has fallen out of favor due to long scan times and poor image quality. In the case of FBI, motion sensitivity in the pelvis and inconsistency in demonstrating vessel segments distal to severe stenotic lesions represent major drawbacks relative to QISS. In terms of spatial resolution, FBI is better than QISS in the craniocaudal dimension but inferior in the anteroposterior dimension. However, no definitive conclusions about relative clinical utility can be inferred until direct comparisons are conducted in patients with PVD.

There are several limitations of this study. First, digital subtraction angiography, the nominal gold standard, was not available for correlation in the pilot study. Second, the patient data analysis was qualitative and we did not quantify vessel diameters and stenosis length. Third, one cannot assume that the imaging parameters found to be optimal in this initial study will prove best for all subjects. It is anticipated that some patients may have a delayed onset or prolonged duration of systole, thereby requiring adjustment of the time delay or QI. Moreover, the field of view may need to be increased in patients with a very large girth. Very tortuous arteries with superiorly directed segments may show signal loss due to the effect of the venous presaturation pulse. Potential solutions include increasing the displacement of the venous presaturation slab from the slice or tilting the slice. Finally, it should be recognized that CE-MRA offers certain advantages compared with current unenhanced methods, such as shorter scan time, the ability to acquire time-resolved images that show flow dynamics, concurrent depiction of the renal arteries, and less artifact from surgical clips and metallic implants. On the other hand, one always has the option with unenhanced MRA techniques to repeat all or part of the data acquisition in case of technical difficulty or patient motion, an option that is not afforded by CE-MRA. With QISS, one can repeat a single slice in one second and an entire slice group in only 1 min. Moreover, for patients with eGFR >30 mL/min/1.73 m^2, one can follow the unenhanced MRA with a CE study if image quality for one or more segments is determined to be unsatisfactory.

In conclusion, QISS MRA is a fast, easy-to-use method for depicting the peripheral arteries. In a small group of patients, this unenhanced technique accurately identified and characterized PVD. Moreover, image quality was consistent irrespective of the disease severity or location. Unlike unenhanced subtractive MRA methods, one does not need to routinely tailor the imaging parameters for each patient. Although the initial clinical results appear promising, a larger cohort will be required to determine the clinical accuracy of the technique.

ACKNOWLEDGMENTS

This work was supported by The Grainger Foundation and 1R01HL096916.

REFERENCES

1. Criqui MH, Fronek A, Barrett-Connor E, Klauber MR, Gabriel S, Goodman D. The prevalence of peripheral arterial disease in a defined population. Circulation 1985;71:510–515.
2. Hiatt WR. Medical treatment of peripheral arterial disease and claudications. N Engl J Med 2001;344:1608–1621.
3. Ersoy H, Rybicki FJ. MR angiography of the lower extremities. AJR Am J Roentgenol 2008;190:1675–1684.
4. Guerrero A, Montes R, Munoz-Terol J, et al. Peripheral arterial disease in patients with stages IV and V chronic renal failure. Nephrol Dial Transplant 2006;21:3525–3531.
5. Kuo PH, Kanal E, Abu-Alfa AK, et al. Gadolinium-based MR contrast agents and nephrogenic systemic fibrosis. Radiology 2007;242: 647–649.
6. Kaufman JA, McCarter D, Geller SC, Waltman AC. Two-dimensional time-of-flight MR angiography of the lower extremities: artifacts and pitfalls. AJR Am J Roentgenol 1998;171:129–135.
7. Owen RS, Carpenter JP, Baum RA, Perloff LJ, Cope C. Magnetic resonance imaging of angiographically occult runoff vessels in peripheral arterial occlusive disease. N Engl J Med 1992;326:1577–1581.
8. McCauley TR, Monib A, Dickey KW, Clemett J, Meier GH, Egglin TK, Gusberg RJ, Rosenblatt M, Pollak JS. Peripheral vascular occlusive disease: accuracy and reliability of time-of-flight MR angiography. Radiology 1994;192:351–357.
9. Miyazaki M, Takai H, Sugiura S, Wada H, Kuwahara R, Urata J. Peripheral MR angiography: separation of arteries from veins with flow-spoiled gradient pulses in electrocardiography-triggered three-dimensional half-Fourier fast spin-echo imaging. Radiology 2003;227: 890–896.
10. Nakamura K, et al. Fresh blood imaging (FBI) of peripheral arteries: comparison with 16-detector row CT angiography. Proc Int Soc Magn Reson Med 2006;14:1929.
11. Lim RP et al. 3D nongadolinium-enhanced ECG-gated MRA of the distal lower extremities: preliminary clinical experience. J Magn Reson Imaging 2008;28:181–189.
12. Fuchs F, Laub G, Othomo K. TrueFISP—technical considerations and cardiovascular applications. Eur J Radiol 2003;46:28–32.
13. Korosec FR, Frayne R, Grist TM, Mistretta CA. Time-resolved contrast-enhanced 3D MR angiography. Magn Reson Med 1996;36:345–51.
14. Wright GA, Nishimura DG, Macovski A. Flow-independent magnetic resonance projection angiography. Magn Reson Med 1991;17: 126–140.
15. Edelman RR, Koktzoglou I. Unenhanced flow-independent MR venography by using signal targeting alternative radiofrequency and flow independent relaxation enhancement. Radiology 2009;250: 236–245.
16. Deimling M, Heid O. Magnetization prepared true FISP imaging. In: Proceedings of the Second Annual Meeting of the Society of Magnetic Resonance, San Francisco, 1994. p 495.
17. Scheffler K, Lehnhardt S. Principles and applications of balanced SSFP techniques. Eur Radiol 2003;13:2409–2418.